Photoisomerization of acetyl methyl iminoxy radical in low-temperature argon matrices studied by density functional theory

ARTICLE *in* CHEMICAL PHYSICS LETTERS · SEPTEMBER 2000

Impact Factor: 1.9 · DOI: 10.1016/S0009-2614(00)00937-4

5 AUTHORS, INCLUDING:

Munetaka Nakata
Tokyo University of Agriculture and Te…

166 PUBLICATIONS **2,151** CITATIONS

29 September 2000

ELSEVIER

Chemical Physics Letters 328 (2000) 283–290

CHEMICAL PHYSICS LETTERS

www.elsevier.nl/locate/cplett

Photoisomerization of acetyl methyl iminoxy radical in low-temperature argon matrices studied by density functional theory

Satoshi Kudoh [a], Tomohiro Uechi [a], Masao Takayanagi [a], Munetaka Nakata [a,*], Heinz Frei [b]

[a] *Graduate School of Bio-Applications and Systems Engineering (BASE), Tokyo University of Agriculture and Technology, 2-24-16 Naka-cho, Koganei, Tokyo 184-8588, Japan*

[b] *Physical Biosciences Division, MS Calvin Laboratory, Lawrence Berkeley National Laboratory, 1 Cyclotron Road, CA 94720, USA*

Received 25 July 2000; received in final form 16 August 2000

Abstract

Photoisomerization of acetyl methyl iminoxy radical produced from NO_2 and 2-butyne in low-temperature argon matrices has been studied by density functional theory (DFT) calculation. The infrared bands observed upon 585 nm irradiation are assigned, using the spectral patterns predicted by DFT, to the *trans–trans*, *cis–trans*, and *cis–cis* conformers, where the former and latter conformations refer to the CO–CN and C=N bond axes, respectively. Conformational isomerization around the C=N bond is found to occur upon 515 nm irradiation. The isomerization mechanism is discussed with the aid of the DFT calculation.

1. Introduction

In visible light-induced bimolecular reactions between NO_2 and various organic compounds in low-temperature argon matrices [1–19], we observed production of acetyl methyl iminoxy radical, 3-oxobutan-2-iminoxyl [11]. The oxygen atom in NO_2 excited electronically by visible radiation is transferred to 2-butyne to produce oxyrene biradical, which is so unstable that it immediately changes to keto carbene. Since a reactive coproduct, NO, exists near keto carbene in an argon matrix, acetyl methyl iminoxy radical is produced by recombination of these species. The reaction mechanism is as shown in Scheme 1.

We reported [11] the infrared bands of three conformers (I_A, I_{B1}, and I_{B2}) of the iminoxy radical generated by 585 nm irradiation. Photoisomerization from I_A to I_{B1} that occurred upon 515 nm irradiation resulted in a decrease in the intensity of I_A and an increase in that of I_{B1}, while that of I_{B2} remained unchanged. The conformers were identified by comparison with the UV-induced photoisomerization of a related compound, 2,3-butanedione monoxime. However, there was no evidence for decisive identification.

Density functional theory (DFT) calculations have been used widely in various fields of molecular science [20–22]. Most of the vibrational wavenumbers predicted by this method are shown

* Corresponding author. Fax: +81-42-388-7349.
E-mail address: necom@cc.tuat.ac.jp (M. Nakata).

0009-2614/00/$ - see front matter
PII: S0009-2614(00)00937-4

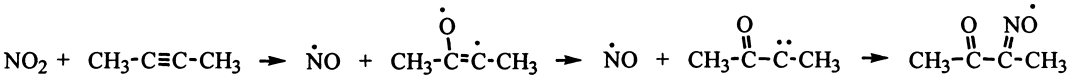

Scheme 1.

to be consistent with the corresponding observed bands within 10 cm^{-1} if a scaling factor is used [23–30]. Thus accurate predictions by DFT have enabled correct identification of conformers among various possibilities no matter whether their spectral patterns are clearly distinguishable from one another. For example, the stable conformers of 1,2-ethanediamine [29] and dimethylaminomethanol [30] have been assigned by DFT calculations. In the present study, we apply this method for prediction of the vibrational wavenumbers of four conformers of acetyl methyl iminoxy radical, shown in Fig. 1, to assign the observed infrared bands of the 50% ^{18}O and ^{16}O species.

2. Experimental and calculation

The experimental details have been reported elsewhere [11]. NO_2 and 2-butyne diluted with argon gas were co-deposited on a CsI plate. The concentration ratio used was 2-butyne/NO_2/Ar = 2.5:1:200. A sample of 50% ^{18}O isotope-substituted NO_2 was prepared by mixing $N^{16}O$ with $^{18}O_2$ in the gas phase. An argon ion laser-pumped CW dye laser (585 nm) was used to produce acetyl methyl iminoxy radical, while a prism-tuned argon ion laser (515 nm) was used to induce photoisomerization of the radical.

DFT calculations were performed by using the GAUSSIAN 98 program [31] with the $6-31++G^{**}$ basis set, where the hybrid density functional [32], in combination with the Lee–Yang–Parr correlation functional (B3LYP) [33], was used to optimize the geometrical structures.

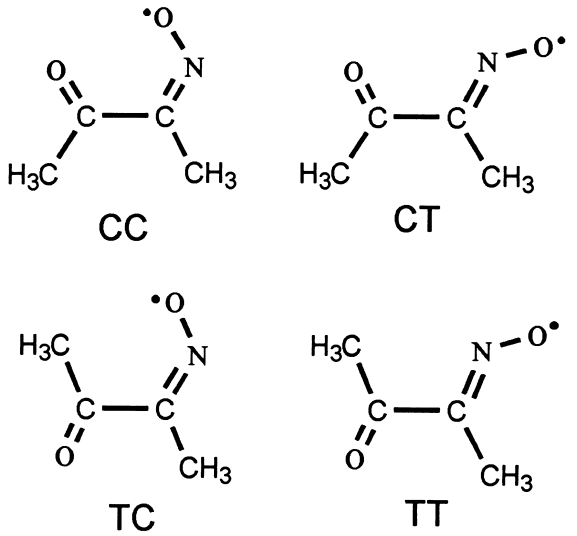

Fig. 1. Four possible conformers of acetyl methyl iminoxy radical.

3. Results and discussion

3.1. Relative energies and optimized geometry

Since acetyl methyl iminoxy radical, $CH_3COCNOCH_3$, has *trans* and *cis* conformations around the CO–CN and C=NO bonds, four conformers, TT, TC, CT, and TT, are possible, as shown in Fig. 1. The optimized geometries obtained by the DFT calculations are planar for all the conformers; their geometrical parameters and relative energies are summarized in Table 1. Conformer TT is shown to be the most stable, while CT is the least stable, probably because of the repulsion between the two lone pairs of the N and O atoms. This repulsion may result in an increase in the O=C–CN angle of CT to exceed 120°. Most of the structural parameters are similar except for those of the C=N–O group of TC; the C=NO and CO–C=N angles of TC are larger than those of the other conformers by about 5°. In addition, the CO–CN bond of TC is longer than that of the other conformers. These findings suggest that the repulsion between the C=N–O group and the methyl group bonded to the C=O carbon cannot

Table 1
Optimized geometry (in Å or degrees) and relative energies (in kJ mol^{-1}) of conformers of iminoxy radical[a]

Conformer	TT	TC	CC	CT
ΔE[b]	−20.08	−14.38	−7.34	0.00
r(N–O)	1.227	1.228	1.225	1.222
r(C=N)	1.296	1.294	1.301	1.297
r(CO–CN)	1.492	1.505	1.497	1.497
r(C=O)	1.223	1.222	1.221	1.221
r(CN–CH_3)	1.505	1.503	1.505	1.511
r(CO–CH_3)	1.515	1.511	1.518	1.518
⟨(C=N–O)	133.0	136.1	131.3	133.8
⟨(CO–C=N)	116.8	121.9	117.5	115.2
⟨(O=C–CN)	119.2	117.5	120.9	121.5
⟨(C–CN–CH_3)	122.0	119.1	123.8	124.0
⟨(CH_3–CO–C)	118.8	119.9	117.1	116.8

[a] Other structural parameters are available upon request.
[b] Relative energies.

be disregarded. Our calculations are fully consistent with those reported by Jaszewski et al. [34], who calculated the relative energies, optimized geometry, and EPR parameters such as isotropic hyperfine coupling constants using various basis sets.

3.2. C=O *and* C=N *stretching modes*

The C=O and C=N stretching modes of acetyl methyl iminoxy radical are expected to appear around 1700 and 1600 cm^{-1}, respectively. The wavenumbers of these bands strongly depend on the conformations around the CO–CN and C=N bonds. Our DFT predictions for the C=O stretching mode of TT, TC, CC and CT, adjusted by a linear scaling function [23], are 1713, 1711,

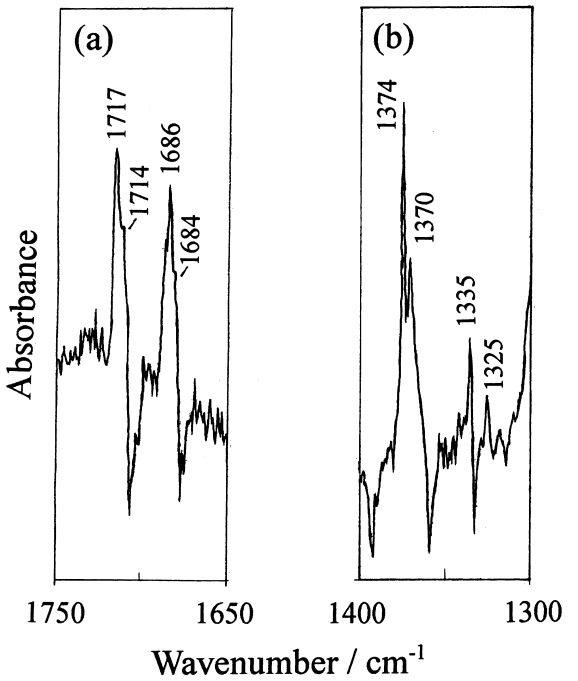

Fig. 2. A difference infrared spectrum of 50% ^{18}O isotope acetyl methyl iminoxy radical obtained upon 515 nm irradiation (85 mW cm^{-2}) for 3 min subsequent to 585 nm irradiation for 5 h. (a) C=O stretching region, (b) N–O stretching region. The decreasing bands are assigned to I_A of CC, and the increasing bands to I_{B1} of CT.

Table 2
Calculated and observed vibrational wavenumbers (in cm^{-1}) of conformers of acetyl methyl iminoxy radical

	Calculated[a]				Observed[b]				
Conformer[c]	$\nu_{C=O}$[d]	$\Delta\nu_{C=O}$[e]	$\nu_{C=N}$[d]	$\Delta\nu_{C=N}$[e]	$\nu_{C=O}$	$\Delta\nu_{C=O}$[e]	$\nu_{C=N}$	$\Delta\nu_{C=N}$[e]	Conformer[f]
TT	1713	0	1623	0	1711	0	1591	0	I_{B2}
TC	1711	−2	1642	+19					
CC	1709	−4	1583	−40	1707	−4	1560	−31	I_A
CT	1720	+7	1629	+6	1717	+6	1600	+9	I_{B1}

[a] Calculated by DFT/B3LYP/6-31++G**.
[b] Observed by matrix-isolation infrared spectroscopy.
[c] See in Fig. 1.
[d] Scaled by a linear function: 0.989–0.0000104ν [23].
[e] Shifts from that of TT.
[f] Ref. [11].

Table 3
Comparison of calculated and observed wavenumbers with significant ^{18}O isotope shifts (in cm^{-1})

Species	$^{16}OC–CN^{16}O$	$^{18}OC–CN^{16}O$	$^{16}OC–CN^{18}O$	$^{18}OC–CN^{18}O$
Wavenumbers	ν	$\Delta\nu$[a]	$\Delta\nu$[a]	$\Delta\nu$[a]
Observed	1717	−31	−3	−33
Calculated (CT)	1720	−27	−2	−31
Calculated (TC)	1711	−29	−2	−33
Observed	1374	0	−4	−4
Calculated (CT)	1372	0	−4	−4
Calculated (TC)	1367	0	0	0
Observed	1335	0	−10	−10
Calculated (CT)	1346	0	−11	−11
Calculated (TC)	1331	0	−21	−21

[a] ^{18}O isotope shifts.

1709, and 1720 cm^{-1}, respectively (see Table 2). The C=N stretching mode shows larger conformer shifts than the C=O stretching mode: the wavenumbers for CC, 1583 cm^{-1}, is significantly lower than those for the other conformers, 1623, 1642, and 1629 cm^{-1}. We observed the relevant bands [11] at 1711 and 1591 cm^{-1} for I_{B2}, 1707 and 1560 cm^{-1} for I_A, and 1717 and 1600 cm^{-1} for I_{B1}. Since the wavenumbers of the C=N stretching mode for I_A is 30 cm^{-1} smaller than those for I_{B1} and I_{B2}, it

Table 4
Observed and calculated wavenumbers of CC conformer (in cm^{-1})

Normal					^{15}N		^{18}O	
ν_{cal}[a]	I_{calc}[a]	ν_{scal}[b]	ν_{obs}[c]	I_{obs}[c,d]	$\Delta\nu_{scal}$[b,e]	Δ_{obs}[c,e]	Δ_{scal}[b,e]	$\Delta\nu_{obs}$[c,e]
1760	1.23	1709	1707	s	−3	−2	−31	−30
1628	2.71	1583	1560	vs	−29	−28	−18	−14
1505	0.05	1466			−1		−2	
1491	0.24	1452			0		0	
1475	0.03	1437			−1		0	
1467	0.22	1429	1426		0	−2	−1	
1432	0.10	1396	1392	w	0	0	−1	−1
1397	0.02	1362	1360	m	−2	−1	−5	0
1380	0.37	1346	1333	s	−4	−4	−14	−18[f]
1271	1.10	1241	1258	s	0	0	−2	
1146	0.58	1120	1131	s	−2	−2	−2	−3
1064	0.00	1041			0		0	
1023	0.03	1001	1004	w	0	0	−1	0
1002	0.05	981	977	w	−4	−5	−5	−2
967	0.43	947	959	s	0	0	−4	−4
699	0.23	687	693	m	−3	−3	−6	0
626	0.17	615	622	s	−4	−4	−5	−6
626	0.02	615			−2		−2	

[a] Calculated by DFT/B3LYP/6-31++G**.
[b] Scaled by a linear function of 0.989–0.0000104ν [23].
[c] Ref. [11].
[d] 'vs', 's', 'm', and 'w' represent very strong, strong, medium, and weak, respectively.
[e] Isotope shifts.
[f] Reassigned in this study.

Table 5
Observed and calculated wavenumbers of CT conformer (in cm^{-1})

Normal					^{15}N		^{18}O	
ν_{calc}[a]	I_{calc}[a]	ν_{scal}[b]	ν_{obs}[c]	I_{obs}[c,d]	$\Delta\nu_{scal}$[b,e]	$\Delta\nu_{obs}$[c,e]	Δ_{scal}[b,e]	$\Delta\nu_{obs}$[c,e]
1771	0.64	1720	1717	s	−4	−1	−31	−33
1676	4.34	1629	1600	vs	−31	−34	−21	−10[f]
1500	0.05	1461			0		−1	
1493	0.02	1454			0		0	
1478	0.21	1440			0		0	
1466	0.12	1428	1421[g]	w	0	0	−1	
1412	0.09	1376	1375	w	0	−1	0	−1
1407	0.29	1372	1373	s	−1	−1	−4	−4[g]
1380	0.38	1346	1335	s	−3	−2	−11	−10[g]
1278	1.43	1248	1261	s	−3	−5	−4	
1132	0.39	1107	1120	s	0	0	−2	0
1050	0	1027			0		−1	
1013	0.04	992	993	w	0	0	0	0
994	0.09	973	963	w	−3	0	−3	−7
968	0.12	948	953	w	0	0	−7	−8
744	0.18	730			−7		−3	
608	0.09	598	608	s	−2	−2	−9	−10
592	0.02	582	603	w	0	−2	−2	−4[g]

[a] See footnote 'a' of Table 4.
[b] See footnote 'b' of Table 4.
[c] See footnote 'c' of Table 4.
[d] See footnote 'd' of Table 4.
[e] See footnote 'e' of Table 4.
[f] Overlapped with NO_2.
[g] Reassigned in this study.

is reasonable to assign I_A to CC. The conformer shifts of other conformers are in approximate agreement with the corresponding observed values if I_{B2} and I_{B1} are assigned to TT and CT, respectively, as shown in Table 2.

3.3. ^{18}O isotope shifts

In order to confirm our assignment for I_{B1}, the spectra of 50% ^{18}O isotope species have been re-analyzed. Fig. 2 shows a difference spectrum of the C=O and N–O stretching modes between the spectra measured before and after 515 nm irradiation followed by production of the iminoxy radical by irradiation at 585 nm for 5 h. The decreasing and increasing bands can be ascribed to I_A and I_{B1}, respectively. These vibrational modes strongly depend on ^{18}O isotope substitution. The C=O stretching band of I_{B1} consists of four peaks appearing at 1717, 1714, 1686 and 1684 cm^{-1}. Since acetyl methyl iminoxy radical has two inequivalent O atoms, four distinguishable isotope species, ^{16}OC–C $N^{16}O$, ^{16}OC–$CN^{18}O$, ^{18}OC–$CN^{16}O$ and ^{18}OC–C $N^{18}O$, are possible. The calculated wavenumbers for these isotope species are 1720, 1718, 1693 and 1689 cm^{-1} for CT and 1711, 1709, 1682 and 1678 cm^{-1} for TC. These isotope shifts are satisfactorily reproduced by the DFT calculation for both CT and TC, as shown in Table 3.

On the other hand, the isotope shifts of the N–O stretching mode of CT and TC are largely different. The N–O stretching mode for TC is essentially a pure normal vibration absorbing at 1331 cm^{-1} with an ^{18}O isotope shift of 21 cm^{-1}, as shown in Table 3. In contrast to TC, the N–O stretching mode for CT is mixed with the methyl-bending mode; this mixing results in the two bands predicted at 1346 and 1372 cm^{-1} that show isotope shifts of 11 and 4 cm^{-1}, respec-

Table 6
Observed and calculated wavenumbers of TT conformer (in cm^{-1})

Normal					^{15}N		^{18}O	
ν_{calc}[a]	I_{calc}[a]	ν_{scal}[b]	ν_{obs}[c]	I_{obs}[c,d]	ν_{scal}[b,e]	$\Delta\nu_{obs}$[c,e]	$\Delta\nu_{scal}$[b,e]	$\Delta\nu_{obs}$[c,e]
1764	0.72	1713	1711	s	−4	−2	−33	−30
1670	4.3	1623	1591	vs	−29	−25[e]	−16	
1487	0.11	1448			0		0	
1484	0.02	1445			0		−1	
1478	0.12	1440	1437	w	0	0	0	
1468	0.16	1430	1430	w	0	0	−1	
1399	0.14	1364	1389	w	0	0	−1	
1398	0.41	1363	1369	s	0	0	0	−1
1379	0.26	1345	1329	w	−5	−2	−21	−10[f]
1314	1.22	1282	1301	vs	−3	−6	−3	
1126	0.47	1101	1116	s	0	0	−1	0
1054	0.01	1031			0		0	
1022	0.03	1000			0		0	
1003	0.2	982	987	m	−2	−2	−4	−5
946	0.09	927	953	w	−1	0	−5	−8
743	0.01	729			−7		−3	
602	0.33	592	598	s	−4	−4	−13	−11
600	0.02	590	591	w	0	−1	−4	−6

[a] See footnote 'a' of Table 4.
[b] See footnote 'b' of Table 4.
[c] See footnote 'c' of Table 4.
[d] See footnote 'd' of Table 4.
[e] See footnote 'e' of Table 4.
[f] Overlapped with NO_x.

tively. The observed isotope shifts, 10 and 4 cm^{-1}, are consistent with the prediction for CT, but not for those for TC, 21 and 0 cm^{-1}. These findings lead to the conclusion that I_{B1} is assignable to CT.

The observed wavenumbers reported in Ref. [11] are compared with the wavenumbers for CC, CT, and TT predicted in the present study in Tables 4–6, as well as the values scaled by using a linear function [23]. The overall consistency between the observed and calculated values is satisfactory, including the ^{15}N and ^{18}O isotope shifts.

3.4. Photoisomerization mechanism

The present assignment of I_A and I_{B1} to CC and CT, respectively, implies that the photoisomerization occurs around the C=N bond upon 515 nm irradiation. In order to account for this isomerization, we assume that a π electron of the C=N bond of CC moves to the N–O bond to generate the C–N=O group in an electronically excited state. Then, conformational isomerization around the C–N single bond occurs, and CT is produced after shift of the electron from N=O to C–N (Scheme 2).

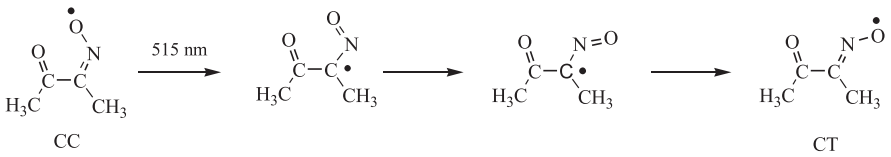

Scheme 2.

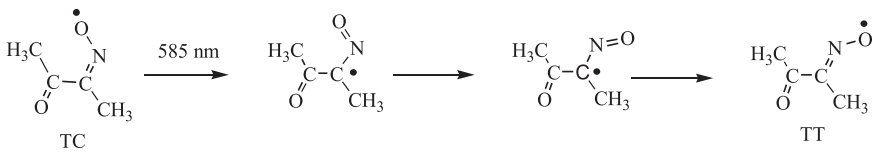

Scheme 3.

In order to confirm this assumption, it will be necessary to obtain further information on the electronically excited state of the iminoxy radical.

Another problem that still remains is as to why the infrared bands of TC are undetectable although this conformer is estimated to be more stable than CC and CT. In order to understand this fact, we assume that all the conformers are produced by 585 nm irradiation and TC is immediately isomerized to TT during the irradiation. Probably TC has a longer absorption wavelength than that of CC. The instant isomerization may also be explained by the prediction that the barrier from the less stable TC to the more stable TT is lower than that from the more stable CC to the less stable CT (Scheme 3).

This assumption will also be verified when further information on the electronically excited states of the iminoxy radical is provided. Recently, Wiberg et al. [35] reported time-dependent density functional theory (TDDFT) and applied it to the electronically excited states of formaldehyde, acetaldehyde and acetone. This method may be applied to explain the mechanism of photoisomerization of the acetyl methyl iminoxy radical.

Acknowledgements

The authors are grateful to Professor Kozo Kuchitsu of Josai University for his helpful discussion.

References

[1] M. Nakata, K. Shibuya, H. Frei, J. Phys. Chem. 94 (1990) 8168.
[2] D.J. Fitzmaurice, H. Frei, J. Phys. Chem. 96 (1992) 10308.
[3] M. Nakata, Y. Somura, M. Takayanagi, N. Tanaka, K. Shibuya, T. Uchimaru, K. Tanabe, J. Phys. Chem. 100 (1996) 15815.
[4] M. Nakata, H. Frei, J. Am. Chem. Soc. 111 (1989) 5240.
[5] M. Nakata, H. Frei, J. Phys. Chem. 93 (1989) 7670.
[6] M. Nakata, H. Frei, J. Chem. Soc. Jpn. (1989) 1412.
[7] D.J. Fitzmaurice, H. Frei, Chem. Phys. Lett. 192 (1992) 166.
[8] M. Nakata, Spectrochim. Acta A50 (1994) 1455.
[9] F. Blatter, H. Frei, J. Phys. Chem. 97 (1993) 3266.
[10] D.J. Fitzmaurice, H. Frei, J. Phys. Chem. 95 (1991) 2652.
[11] M. Nakata, H. Frei, J. Am. Chem. Soc. 114 (1992) 1363.
[12] N. Tanaka, Y. Kajii, K. Shibuya, M. Nakata, J. Phys. Chem. 97 (1993) 7048.
[13] J.A. Harrison, H. Frei, J. Phys. Chem. 98 (1994) 12142.
[14] J.A. Harrison, H. Frei, J. Phys. Chem. 98 (1994) 12152.
[15] N. Tanaka, M. Nakata, K. Shibuya, J. Photochem. Photobiol. 106 (1997) 113.
[16] N. Tanaka, J. Oike, Y. Kajii, K. Shibuya, M. Nakata, Chem. Phys. Lett. 97 (1993) 70.
[17] N. Tanaka, J. Oike, K. Shibuya, M. Nakata, J. Phys. Chem. 100 (1996) 4873.
[18] N. Tanaka, J. Oike, K. Shibuya, M. Nakata, Res. Chem. Intermed. 8 (1998) 893.
[19] S. Kudoh, T. Uechi, M. Takayanagi, M. Nakata, N. Tanaka, K. Shibuya, J. Mol. Struct. 524 (2000) 61.
[20] T. Ziegler, Can. J. Chem. 73 (1995) 743.
[21] J. Labanowski, J.W. Andzelm, Density Functional Methods in Chemistry, Springer, New York, 1991.
[22] J.M. Seminario, P. Politzer, Modern Density Functional Theory: A Tool for Chemistry, Elsevier, Amsterdam, 1995.
[23] S. Kudoh, M. Takayanagi, M. Nakata, Chem. Phys. Lett. 322 (2000) 363.
[24] S. Kudoh, M. Takayanagi, M. Nakata, J. Photochem. Photobiol. A: Chemistry 123 (1999) 25.
[25] S. Kudoh, M. Takayanagi, M. Nakata, Chem. Phys. Lett. 308 (1999) 403.
[26] S. Kudoh, M. Takayanagi, M. Nakata, J. Mol. Struct. 475 (1999) 253.
[27] S. Kudoh, K. Onoda, M. Takayanagi, M. Nakata, J. Mol. Struct. 524 (2000) 61.
[28] S. Kudoh, M. Takayanagi, M. Nakata, J. Mol. Struct. 413/414 (1997) 365.
[29] S. Kudoh, M. Takayanagi, M. Nakata, T. Ishibashi, M. Tasumi, J. Mol. Struct. 479 (1999) 41.
[30] S. Kudoh, M. Takayanagi, M. Nakata, N. Tanaka, K. Shibuya, J. Mol. Struct. 524 (2000) 251.

[31] GAUSSIAN 98, M.J. Frisch, et al., Gaussian, Inc., Pittsburgh, PA, 1998.
[32] A.D. Becke, J. Chem. Phys. 98 (1993) 5648.
[33] C. Lee, W. Yang, R.G. Parr, Phys. Rev. B37 (1988) 785.
[34] A.R. Jaszewski, J. Jezierska, A. Jezierski, Chem. Phys. Lett. 319 (2000) 611.
[35] K.B. Wiberg, R.E. Stratmann, M.J. Frisch, Chem. Phys. Lett. 297 (1998) 60.